**ASSESSING THE SEASONAL WINDS THAT DRIVE REVERSING SAND DUNES AT HELLESPONTUS MONTES, MARS.** M. Chojnacki[1], D. A. Vaz[2], S. Silvestro[3,4], I. B. Smith[1]. [1]Planetary Science Institute, Lakewood, CO (mchojnacki@psi.edu); [2]Centre for Earth and Space Research of the University of Coimbra, Coimbra, Portugal; [3]INAF Osservatorio Astronomico di Capodimonte, Napoli, Italy; [4]SETI Institute, Mountain View, CA.

**Introduction and motivation:** Much of our knowledge about aeolian bedform (dunes and ripples) migration on Mars is thanks to repeat targeting by the HiRISE (*1*) camera. Prior bedform surveys have focused on barchan or transverse dunes (*2*, *3*), as their displacements in a single direction tend to be easiest to quantify. These dunes form under unidirectional or bimodal winds but with a divergence angle (the angle between the two winds) less than 90° (*4*). In comparison, some dunes and dune fields are subject to multi-directional wind regimes (orthogonal or converging) that are encapsulated within a single HiRISE sequence (~5-6 km by ~5-15 km). Locally, longitudinal or oblique dunes develop when the divergence angle is >100° (*4*), but more broadly the dominant wind regime can vary for different zones of a dune field. Although these more complex dunes have been examined in terms of morphology (*5*), their dynamics have largely been unexplored.

The goal of this project is to characterize and explain how Martian aeolian bedform systems evolve spatially and temporally under seasonally (and directionally) variable winds. Related questions we address are how temperature variations and basin-scale topography impact sand transport.

**Study sites:** Here we conducted analysis at several sites across Hellespontus Montes (**Fig. 1**). The primary ~20-km-long dune field is located at the flank of the western rim of Hellas (*5*)(**Fig. 1A**; 45.4°E, 41.5°S), where the effects of a multidirectional wind system were earlier described (*3*, *5*, *6*). Dunes and ripples here migrate under at least two main wind regimes (**Fig. 1B** cyan and white; WSW winds in GIF A and ESE wind in GIF B).

**Data sets and methods:** Three objectives are being conducted on these sites. First, displacement measurements were recorded by mapping polylines along the brink of each lee face in *GIS* (*7*, *8*). Along with height estimates from HiRISE topography this approach allows dune migration, sand flux, and azimuth metrics to be systematically quantified (*9*). This included records of long-term migration (6 Mars years) that establish the cumulative effects of different seasonal wind regimes. The second objective examines ripple dynamics in seasonal HiRISE orthoimages (7 images separated by ~22-197° of $L_s$) over Mars years (MY) 34-36 using the *COSI-Corr* tool suite (*10*). A third objective will constrain the seasonal winds at this site using Laboratoire de Météorologie Dynamique (LMD) Global Circulation Models (GCM; (*11*)) and Martian Mesoscale Model (MMM) simulations – note, MMM results will not be presented here.

**Results:** *Bedform morphology and directional trends*: Barchans dominate on the edges of the dune field (**Fig. 1C**) and grade into barchanoid dunes, as sand

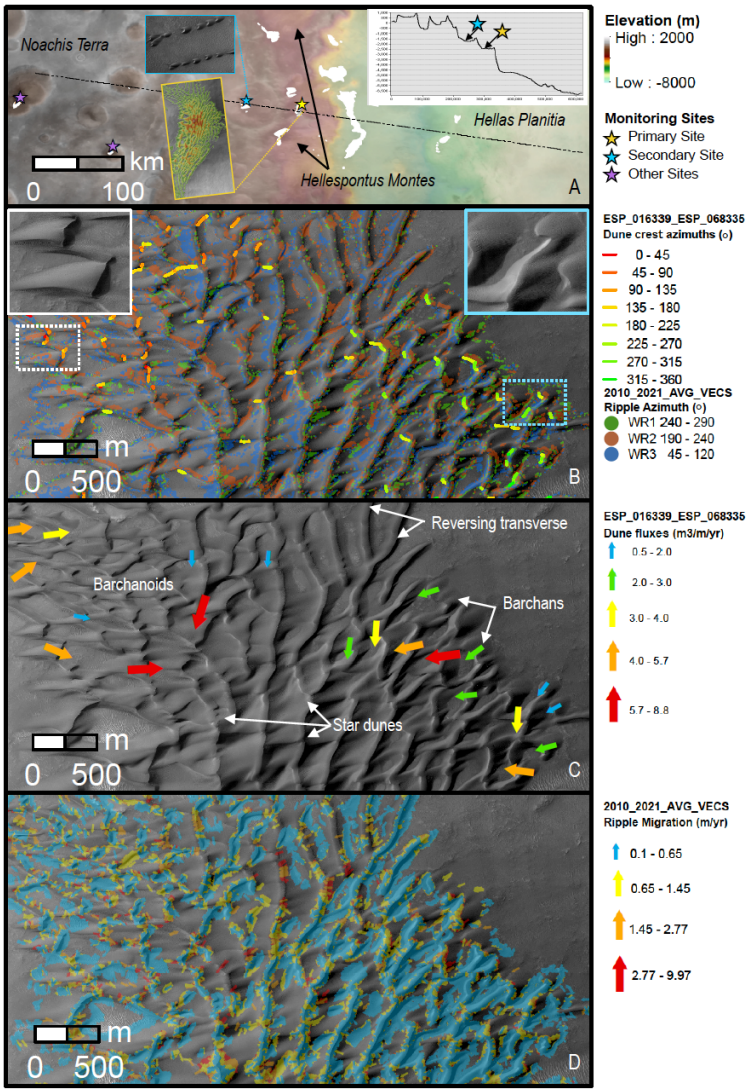


**Figure 1.** A) Context for this study with the primary site (yellow star, Fig. 1B-1D), other active bedform sites (stars), and dune fields in white. HiRISE views (insets) are show. MOC colorized with MOLA elevation, including profile (inset). B) Bedform directional trends from dune motion (color-coded lines) and COSI-Corr ripple displacements (transparent colored circles) over HiRISE ESP_016339_1380. Insets (white and cyan 500 m-wide subareas) show converging dunes migrating E and SW. C) Dune crest flux results from Mars years 30-36. D) Average COSI-Corr ripple migration rates from multiple annual and seasonal images.

supply increases. Some of these occurrences may develop secondary slip faces oriented perpendicular (south) to the primary face. Star dunes with 3 or 4 arms occur in the central areas, while transverse dunes occur in the northeast part of the field.

Dune crest migration patterns over long baselines (MY 30-36) indicate at least 3 converging wind regimes (WR) occur here (**Fig. 1B**, **2A**): (in decreasing influence) WR1) eastern/northern dunes migrating toward the W-WNW (~270°); WR2) dunes in the south are dominantly trending to the SW-SSW; WR3) western dunes migrate toward the E-SE (~95°). Averaged COSI-Corr ripple migration patterns largely confirm these trends with ripples migrating to the W, SW, or E. Megaripples (slower bedforms that respond to longer term winds (*8*)) were also found to be variable in their orientation and migration as influenced by WR1 and WR3.

*Bedform dynamics*: Dune migration rates for the 4 annual time steps converge to ~0.3 m/yr and fluxes range between 2.0-2.7 $m^3$/m/yr, but vary within the dune field (**Fig. 1C**). Fluxes appear to be higher on the eastern side of the field suggesting stronger westward flow – consistent with regional dune morphology (*5*) and transport (*3*). Complicated dune dynamics are observed in central areas with oblique or reversing dune motion, as a given dune may have multiple active slip faces. In contrast, perimeter areas host more symmetric dunes that display transverse motion, indicating the extremely localized impact of various wind regimes.

All three wind regimes are evident in seasonal mapping, depending on the location, slope, or aspect angle. Most (4/6) of the seasonal periods produce ripple migration rates of 3.5-3.7 m/yr. The notable deviations occur within southern autumn-winter ($L_s$ 11-208°) and early summer ($L_s$ 269-312°) (**Fig. 2B**). The earlier and longer period shows the lowest rates related to WR1-WR2, while the far shorter period shows the highest rates driven by WR3. Ripples here often display oblique and longitudinal migration trends which denote the integration of different wind regimes (*7*).

LMD GCM wind modeling here yields steady and strong westward (WR1) winds with a southward bias (WR2) in afternoons/evening year-round (**Fig. 2C**). These are opposed by moderate eastward (WR3) winds throughout the early hours of southern spring-summer. This shift in sand transport also coincides with the transition to the warmer seasons (**Fig. 2C**).

**Discussion:** Hellas basin slope winds, both anabatic and katabatic, have a prominent role in the reversing seasonal sediment transport across Hellespontus. The more common westward sand migration is attributed to persistent up-slope winds out of Hellas (*12*). That trend is offset by eastward winds and sand motion following southern solstice that are bolstered by the higher temperatures and peak heating around perihelion (**Fig. 2C**). Although that combination is responsible for the convergence of sand flow and reversing dune motion in some areas, it can be extremely localized and can be muted by topography. For example, adjacent unidirectional dunes to the west are dominantly westward migrating (**Fig. 1A**, cyan star) and lack evidence for WR3. Thus, winds and sand motion across Hellespontus relate to seasonal temperatures, topography, and location flanking Hellas including its role forming dust storms.

**Acknowledgments:** This research was supported in part by NASA MDAP Grant 80NSSC21K1096. D. V. acknowledge CITEUC's support (UID/Multi/00611/2020).

**References:** [1] McEwen A.S. et al. (2007) JGR, 112, 2005JE002605. [2] Bridges N. et al. (2013) Aeolian Res., 9, 133–151. [3] Chojnacki M. et al. (2019) Geology, G45793.1. [4] Rubin D.M. & H. Ikeda, H. (1990) Sedimentology, 37, 673–684. [5]. Fenton L. et al. (2005) JGR, 110, 2005JE002436.6. [6] Chojnacki M. et al. (2022) 7th IPDW, 3029. [7] Vaz D. et al. (2017) Aeol. Res. 26, 101–116. [8] Silvestro S. et al. (2020) JGR, 112, 2020JE006446. [9] Urso A. et al. (2018) JGR, 123, 353-368. [10] Ayoub F. et al. (2014) Nat. Comm. 5, 10.1038/ncomms6096.[11] Forget F. et al. (1999) JGR, 104, 24155–24175. [12] Fenton L. & M. Richardson (2001) JGR, 106, 32885–32902.

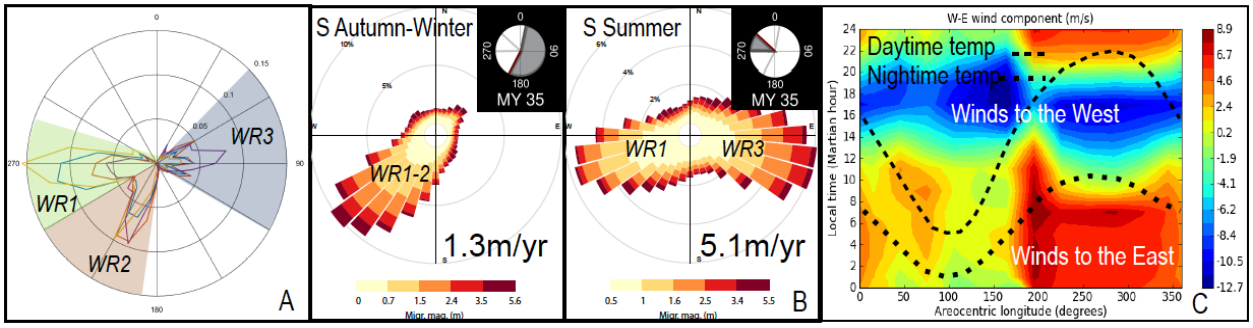


**Figure 2**. A) Dune crest sand flux rose diagram showing 4 annual time steps between MY 30-36. Interpreted wind regimes WR1-3 are overlaid in color. B) COSI-Corr sand rose diagrams for ripples in MY 35 S. Autumn-Winter (left) and early S. Summer (right). Solar longitude plots (upper right) and mean migration rate (lower right) are provided. C) The annual W-E components of surface winds for Hellespontus where warm colors are eastward winds (positive magnitude) and cooler colors are westward winds (negative). LMD GCM atmospheric model. Average TES surface temperatures (black dashed lines) are overlaid that range between 145-305 K.